3 Experimental

Initially, two proprietary samples of graphite were used in this study. The samples had an unknown history, except for the specification that one was a natural material and one was synthetically produced. In addition, both were to be utilised in a nuclear application and it was therefore presumed that both were of very high purity. These samples were given the designations NNG and NSG respectively. Over time it became clear that they were unsuited for an investigation into the mechanisms that govern the oxidation of graphite for a variety of reasons, which will be discussed in subsequent sections.

Four additional graphite samples were therefore studied in an effort to gain insights into the oxidation mechanism. These included two natural graphite samples, namely a flake graphite mined in Zimbabwe of unknown purity (ZNG) and a second flake graphite mined in Germany by Graphit Kropfmühl AG (RFL). The latter was purified with an acid treatment and a high-temperature soda ash burn up to a purity of 99.91%. The material had a specific surface area of 0.8 m^2/g. The particle size distribution is given in Table 3-1.

Table 3-1: Particle size distribution for RFL graphite

%	µm
25	315
48	200
20	160
6	100
1	< 100

In an effort to further purify the RFL graphite samples, they were subjected to high-temperature heat treatments. These treatments were conducted in a TTl furnace (Model: 1000-2560-FP20). Initially, the material was heated to 2 400 ºC in instrument grade (IG) helium, soaked for 3 h and rapidly cooled. However, it was found that this induced excessive pitting in the material, so the cooling rate was reduced to below 1 ºC/min in accordance with the findings of Hennig [318]. Upon oxidation it was found that at high conversions catalytic activity was still visible. This meant that this material was only partially purified and it was designated PPRFL. Finally, the RFL material was subjected to a 6 h soak at 2 700 ºC, followed by slow cooling. This was found to fully purify the material with

no visible catalytic activity even at very high conversions. This material was designated PRFL. In an effort to investigate the effect of a known channelling catalyst on the purified material, a subsample of the PRFL material was soaked in demineralised water containing 250 ppm sodium carbonate. This purified material, which was recontaminated with one specific catalyst, was designated CPRFL.

A second synthetic graphite material with an unknown history was obtained from Fluka Chemical Suppliers (FSG). Finally, a few flakes (ca. 1 mm in diameter) of synthetically derived, highly crystalline Kish graphite (KISH) were also analysed. All SEM images were obtained using an ultra-high resolution field-emission SEM (HR FEGSEM Zeiss Ultra Plus 55) with an InLens detector at acceleration voltages as low as 1 kV to ensure maximum resolution of surface detail. These images are discussed extensively in Chapter 4.

The powder X-ray diffraction (PXRD) spectra of the graphite samples were obtained using a PANalytical X-pert Pro powder diffractometer with variable divergence and receiving slits, and an X'celerator detector using iron-filtered cobalt Kα radiation. They are presented as variable slit data since this allows better data visualisation, as shown in Figure 3-1 to Figure 3-6, with the intensity plotted on a logarithmic scale. The PXRD spectra of as-received RFL natural graphite and fully purified, heat-treated RFL (PRFL) are practically identical, indicating that no modification of the crystal structure took place during the heat treatment.

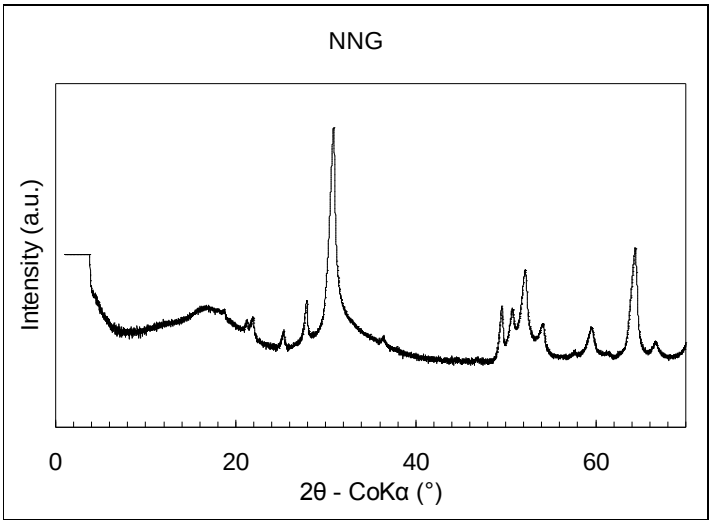

Figure 3-1: XRD spectrum of NNG graphite

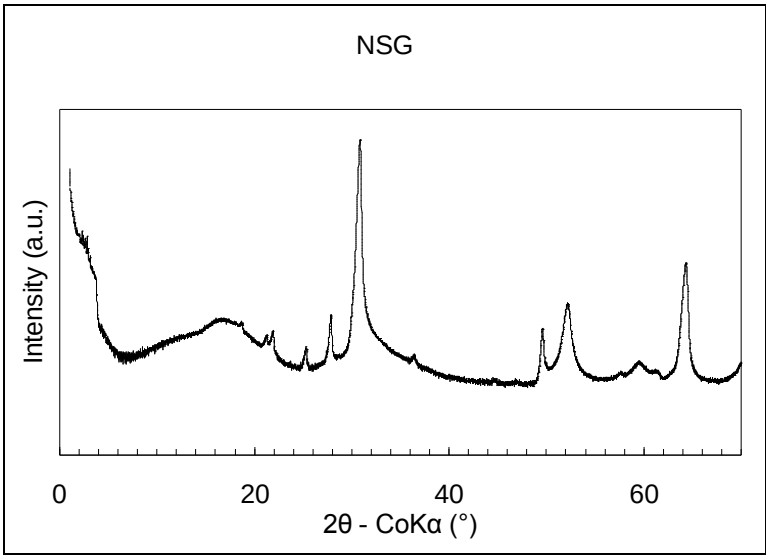

Figure 3-2: XRD spectrum of NSG graphite

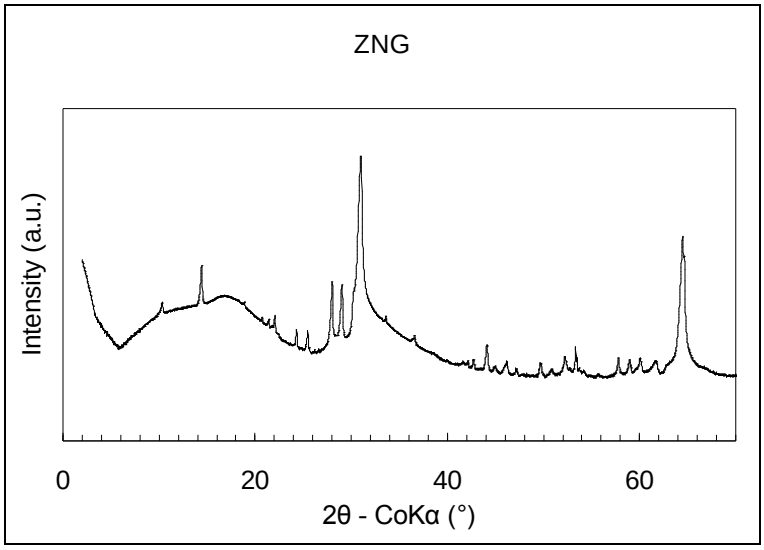

Figure 3-3: XRD spectrum of ZNG graphite

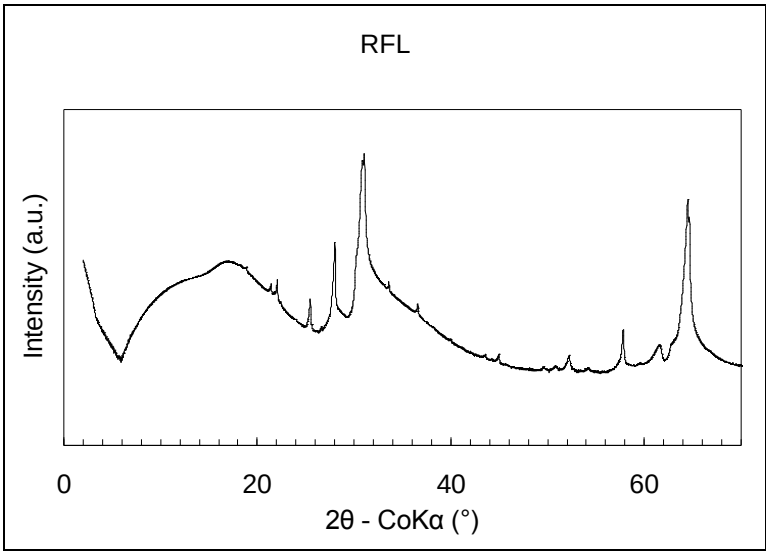

Figure 3-4: XRD spectrum of RFL graphite

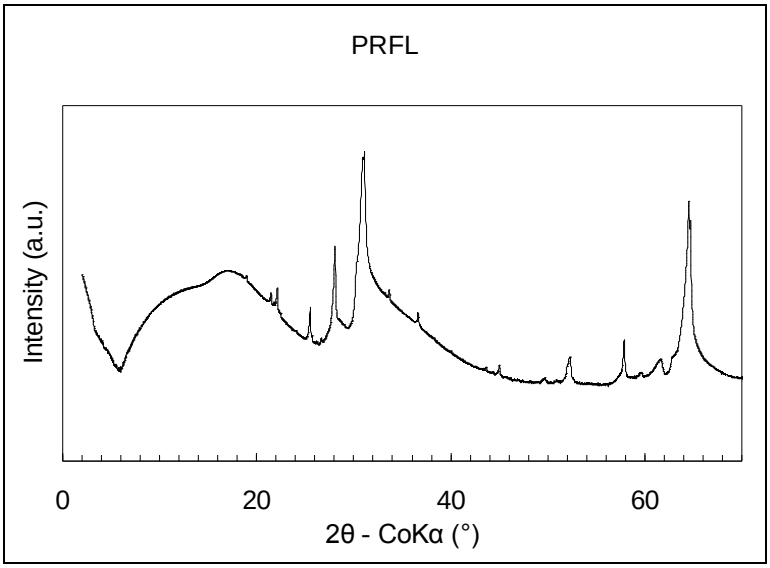

Figure 3-5: XRD spectrum of PRFL graphite

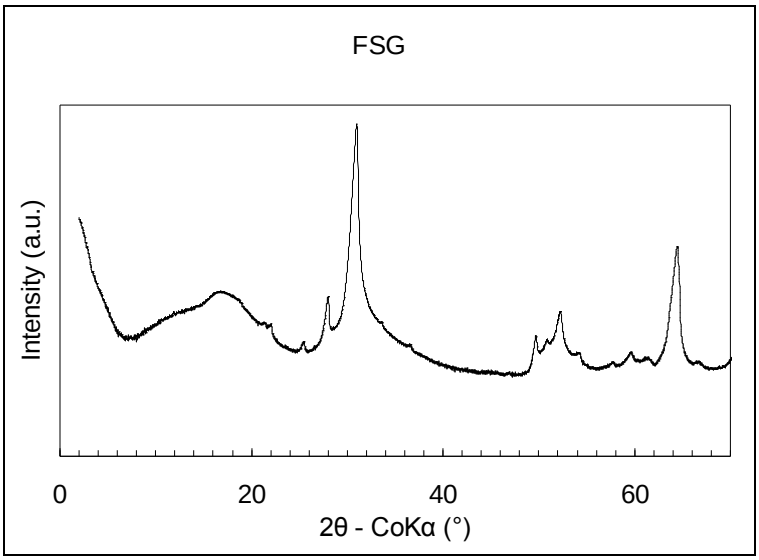

Figure 3-6: XRD spectrum of FSG graphite

Raman spectra of the NNG and NSG samples were obtained using a Dilor XY Raman spectrometer using the λ = 14.3 nm laser line of a coherent Innova 90 Ar^{+}-laser. These spectra are shown in Figure 3-7 in Figure 3-8 respectively.

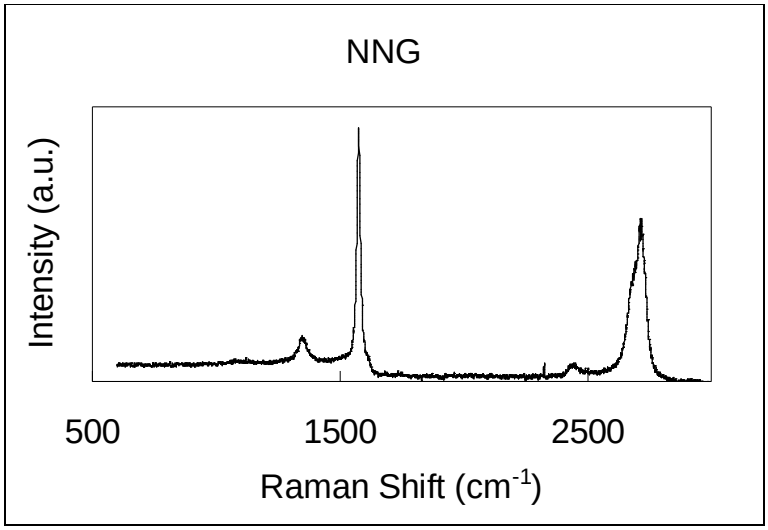

Figure 3-7: Raman spectrum of NNG graphite

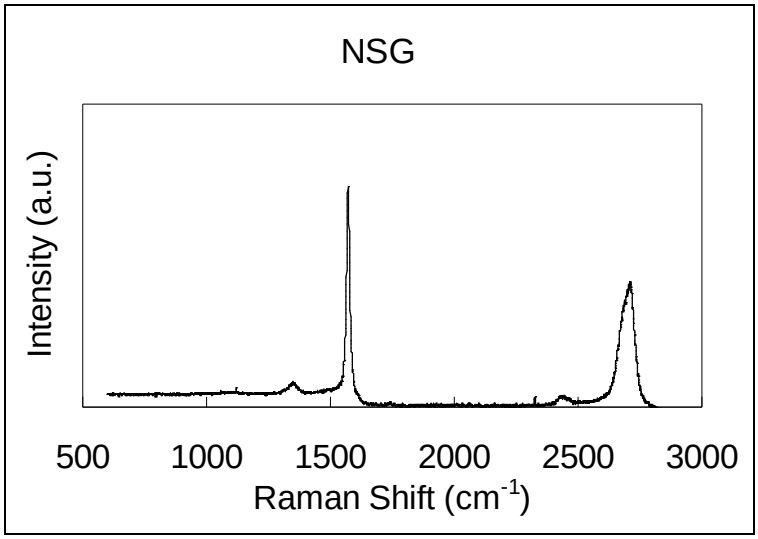

Figure 3-8: Raman spectrum of NSG graphite

The BET surface areas of the NNG and NSG samples were found to be 0.88 and 0.96 m^2/g respectively, using a Quantachrome Nova surface area analyser. Furthermore, the densities for both samples were found to be approximately equal to the ideal crystal density, i.e. 2.26 g/cm^3, indicating that the samples had very little or no porosity. In an effort to characterise the surface groups present on the graphite, XPS, DRIFT and TPD were attempted. None of these methods delivered tangible results. This is not unexpected given the very low surface areas of the samples. The apparent particle size distributions (PSDs) of the NNG and NSG samples were obtained on a Malvern Mastersizer Hydro 2000MY instrument. These are shown in Figure 3-9.

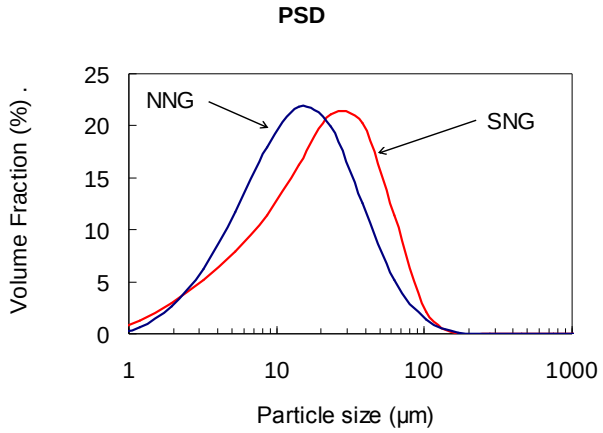

Figure 3-9: Particle size distribution of NNG and NSG graphite

The impurity contents of the samples were analysed using an ARL9400 XP+ Sequential XRF analyser and Uniquant software. The compositions are shown in Table 3-2. The analysis was done for all elements in the periodic table between Na and U, but only elements found above the detection limits are reported. The carbon is calculated by difference. Due to the nature of the analysis, a variable amount of oxygen is also detected, possibly caused by sample porosity. Since the carbon is calculated by difference, the oxygen was omitted but this adjustment makes the absolute value of the percentage carbon unreliable, indicating that it should be used only as a qualitative value.

Table 3-2: XRF compositional analysis (Mass %)

	NNG	SNG	ZNG	RFL	PRFL	FSG
Si	0.01	0.01	1.49	0.01	*<0.01*	0.01
Ti	*<0.01*	*<0.01*	0.02	*<0.01*	*<0.01*	0.01
Al	*<0.01*	*<0.01*	0.90	*<0.01*	*<0.01*	*<0.01*
Fe	*<0.01*	*<0.01*	0.48	0.01	*<0.01*	0.01
Mg	0.02	0.01	0.11	0.04	0.03	0.01
Ca	*<0.01*	*<0.01*	0.10	*<0.01*	*<0.01*	0.01
Na	0.10	0.02	0.04	0.09	0.02	0.06
K	*<0.01*	*<0.01*	0.10	*<0.01*	*<0.01*	*<0.01*
P	*<0.01*	*<0.01*	0.01	*<0.01*	*<0.01*	*<0.01*
S	0.06	0.01	0.17	0.02	0.01	0.03
Mo	0.01	0.01	0.01	*<0.01*	*<0.01*	0.01
Th	*<0.01*	0.01	*<0.01*	*<0.01*	*<0.01*	*<0.01*
Carbon	99.81	99.95	96.57	99.83	99.95	99.87

The purified RFL material (PRFL) shows a clear reduction in impurity content when compared with the as-received material (RFL). The PRFL and the SNG material show the lowest impurity levels (< 500 ppm), very close to the detection limits of this particular XRF and measurement procedure. Furthermore, during the SEM examination, EDS spectroscopy of individual impurities found in the RFL graphite sample was conducted using an Oxford Instruments NanoTrace detector. The image of the impurity under consideration, highlighted in red, is shown first (Figure 3-10, Figure 3-12, Figure 3-14, Figure 3-16 and Figure 3-18) and the corresponding EDS spectrum is shown in the following figure (Figure 3-11, Figure 3-13, Figure 3-15, Figure 3-17 and Figure 3-19).

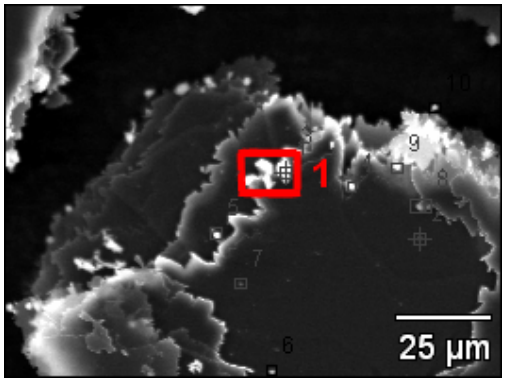

Figure 3-10: SEM image of impurity 1 found on RFL graphite

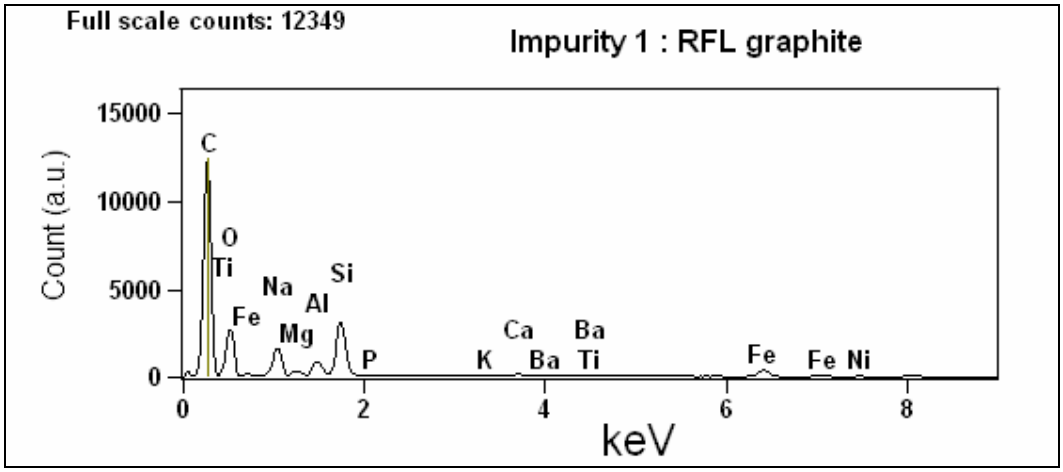

Figure 3-11: EDS spectra of impurity 1 found on RFL graphite

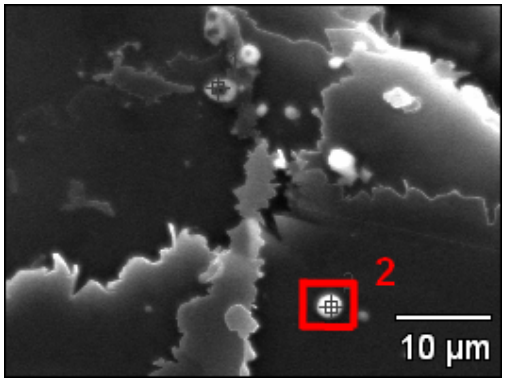

Figure 3-12: SEM image of impurity 2 found on RFL graphite

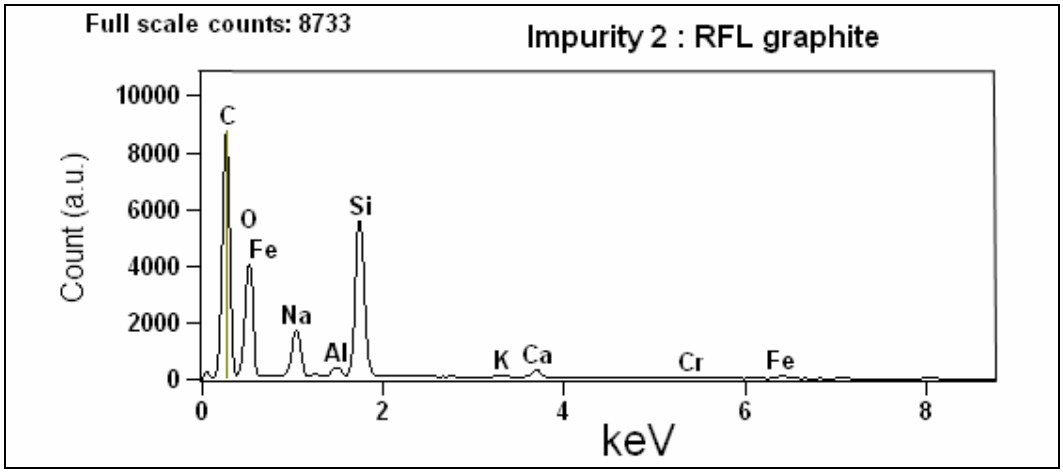

Figure 3-13: EDS spectra of impurity 2 found on RFL graphite

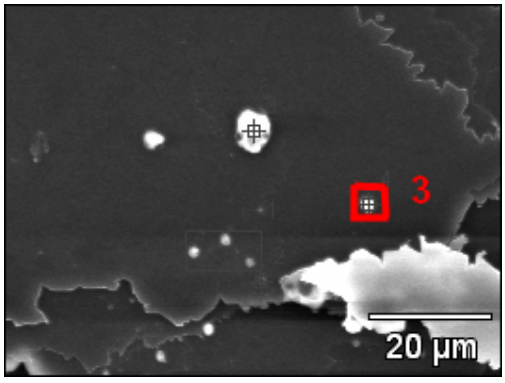

Figure 3-14: SEM image of impurity 3 found on RFL graphite

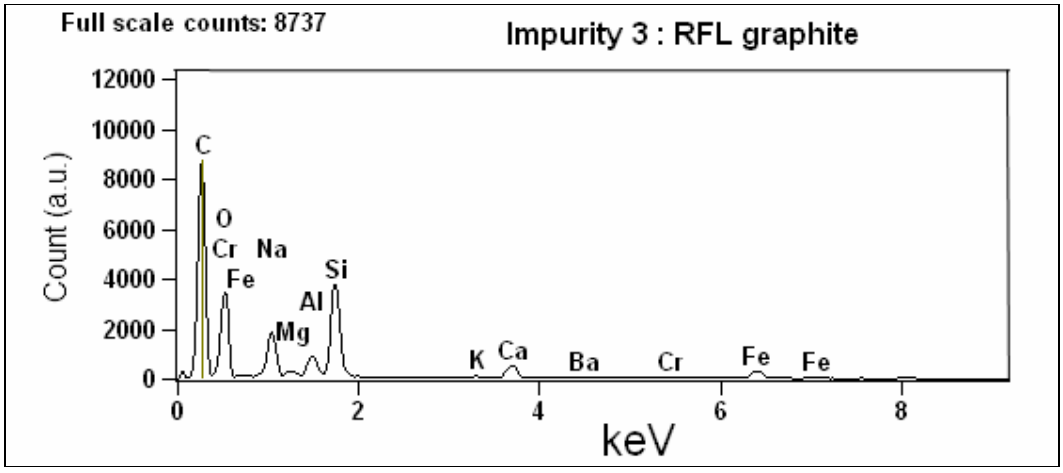

Figure 3-15: EDS spectra of impurity 3 found on RFL graphite

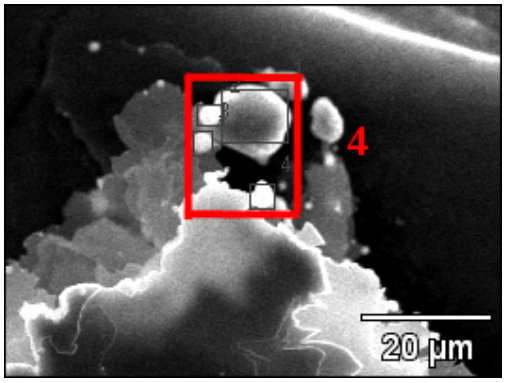

Figure 3-16: SEM image of impurity 4 found on RFL graphite

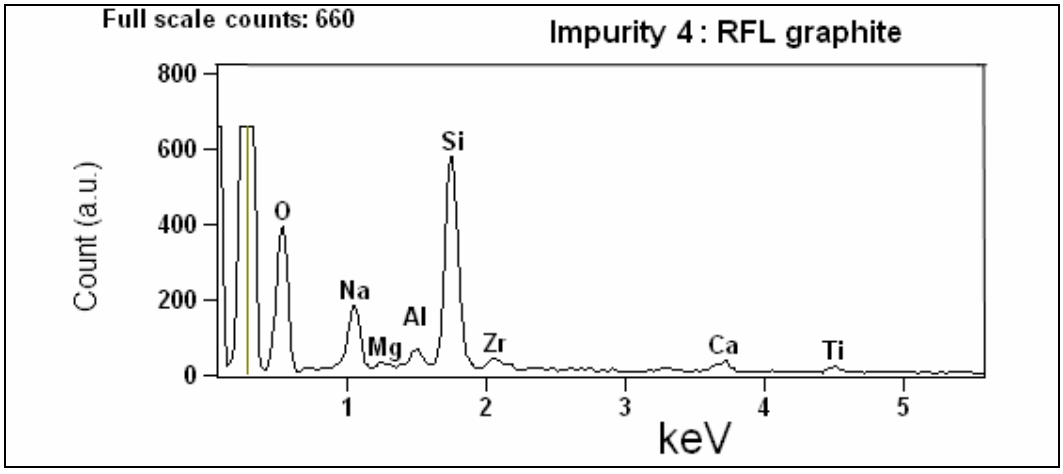

Figure 3-17: EDS spectra of impurity 4 found on RFL graphite

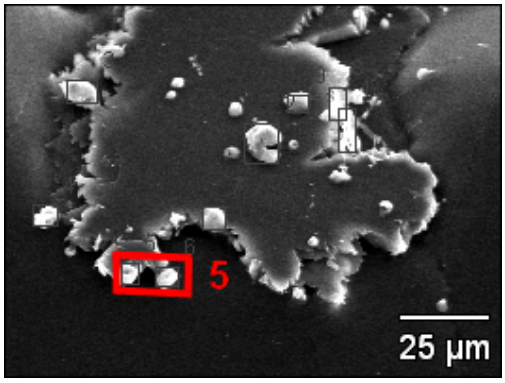

Figure 3-18: SEM image of impurity 5 found on RFL graphite

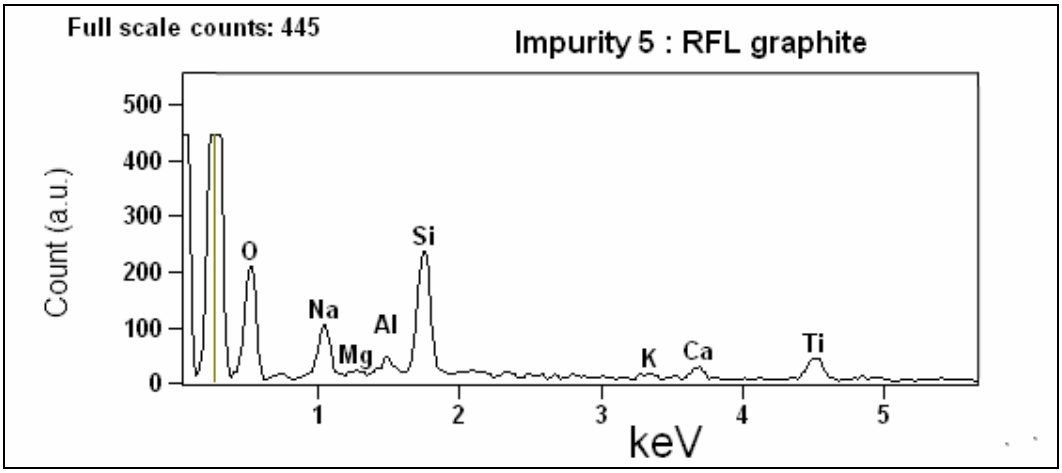

Figure 3-19: EDS spectra of impurity 5 found on RFL graphite

Finally, all thermal analysis was conducted in a TA Instruments SDT Q600 thermogravimetric analyser. Oxidation was performed in IG oxygen, or air in some cases, at various isothermal temperatures. The samples (ca. 1–3 mg) were heated in platinum pans at a scan rate of around 50 ºC/min in IG argon flowing at 300 ml/min, from 25 ºC to temperatures between 600 and 850 ºC. When the desired reaction temperature had been achieved, the temperature was allowed to stabilise for 15 min and then the argon flow was shut off and IG oxygen flow was started at 500 ml/min. For the non-isothermal experiments, samples were heated in the oxidising gas, flowing at 500 ml/min, at a variety of heating rates from 25 ºC to 1 000 ºC. The exact purge gas compositions are given in Table 3-3.

Table 3-3: Purge gas compositions

Air (IG)			**Argon (IG)**			**Oxygen (IG)**		
O_2	21	%	Min. purity	99.999	%	Min. purity	99.5	%
N_2	Balance		O_2	<3	ppm	Argon	<30	vpm
H_2O	<25	ppm	H_2O	<3	ppm	N_2	<200	vpm
CO_2	<500	ppm	CO_2	<1	ppm	CO_2	<300	vpm
CO	<10	ppm	CO	<1	ppm	CO	<5	vpm
			HC	<1	ppm			

The purge gas outlet was connected to a Pfeiffer QMS 200 mass spectrometer. During an empty control experiment, the dynamics of the gas change, from inert to reactive, were found to be quick and characterised by a

first-order process with a time constant of $\tau' \approx 2.6$ min. Based on a single isothermal experiment, the ash content of the samples could be determined by fully oxidising the carbon. The ash contents for all the graphite samples used in this study are shown in Table 3-4.

Table 3-4: Ash content of graphite samples

Sample	%
NNG	<0.1
NSG	<0.1
ZNG	15
RFL	<0.1
FSG	1-2
KISH	<0.1